Visual Motion Observer-based Stabilizing Receding Horizon Control via Image Space Navigation Function

Toshiyuki Murao, Hiroyuki Kawai and Masayuki Fujita

Abstract— This paper investigates stabilizing receding horizon control via an image space navigation function for a three-dimensional (3-D) visual feedback system. Firstly, a brief summary of a visual motion observer is given. Next, a visual motion error system is reconstructed in order to apply to time-varying desired motion. Then, visual motion observer-based stabilizing receding horizon control for the 3-D visual feedback system, highly nonlinear and relatively fast system, is proposed. Moreover, a path planner to be appropriate for the visual motion error system is designed through the image space navigation function to keep all features into a camera field of view. Finally, simulation results are shown in order to confirm the proposed method.

I. INTRODUCTION

Visual feedback control is now a very flexible and useful method in robot control [1]. Recently, Gans and Hutchinson [2] proposed hybrid switched-system control which utilizes image-based and position-based visual feedback control. In [3], an occlusion problem for a hybrid eye-in-hand/eye-to-hand multicamera system was tackled by using an extended Kalman filter and a multiarm robotic cell.

Especially, there has been an increase of interest in problems that are all feature points remain within a camera field of view since the work of Chaumette [4], while many researchers have tackled various problems for visual feedback control. Cowan *et al.* [5] proposed a visual feedback controller to bring a robot to rest at a desired configuration for the field of view problem by using navigation functions, similar to artificial potential functions. Chen *et al.* [6] developed an off-line path planner based on an image space navigation function with an adaptive 2 1/2-D visual servoing controller. However, the desired control performance cannot be guaranteed explicitly, since these control methods [5], [6] are not based on optimization.

On the other hand, receding horizon control, also recognized as model predictive control is a well-known control strategy in which the current control action is computed by solving a finite horizon optimal control problem on-line [7]. Sauvée *et al.* [8] proposed an image-based visual servoing scheme based on nonlinear model predictive control for robot systems. Allibert *et al.* [9] has been tested it on a planar manipulator arm equipped with an omnidirectional camera in simulation. Although good receding horizon control approaches for the visual feedback system considering the mechanical and visibility constraints are reported in those
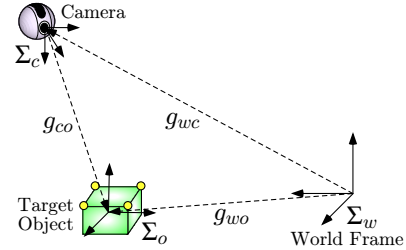
Fig. 1. Eye-in-hand visual feedback systems.

papers, stability does not addressed. In [10], the authors proposed stabilizing receding horizon control for an eye-in/to-hand visual feedback system which includes both an eye-in-hand system and an eye-to-hand one as the special cases. However, this position-based visual feedback control method through nonlinear receding horizon approach can allow feature points to leave the field of view.

In this paper, stabilizing receding horizon control via an image space navigation function is applied to a three-dimensional (3-D) visual feedback system with an eye-in-hand configuration as shown in Fig. 1, highly nonlinear and relatively fast system. Firstly, an brief summary of a visual motion observer is given. Secondly, a visual motion error system is reconstructed in order to handle time-varying desired motion. Next, stabilizing receding horizon control for the visual motion error system using a control Lyapunov function is proposed. Then, a path planner to be appropriate for the visual motion error system is designed through an image space navigation function in order to keep all features into a camera field of view. The path planning based on an image space could be of significant benefit when used in conjunction with the proposed position-based receding horizon control by using an error defined on a Cartesian space. Finally, control performance with visibility maintenance of the proposed control scheme and the previous one [10] is evaluated through simulation results.

II. VISUAL MOTION OBSERVER

This section mainly reviews our previous work [11] via passivity-based visual feedback control with the eye-in-hand configuration.

A. Body Velocity of Relative Rigid Body Motion

Visual feedback systems with the eye-in-hand configuration use three coordinate frames which consist of a world frame Σ_w, a camera frame Σ_c, and an object frame Σ_o as in Fig. 1. Let $p_{co} \in \mathcal{R}^3$ and $e^{\hat{\xi}\theta_{co}} \in SO(3)$ be a position vector and a rotation matrix from the camera frame Σ_c to the object frame Σ_o. Then, the relative rigid body motion from Σ_c to Σ_o can be represented by $g_{co} = (p_{co}, e^{\hat{\xi}\theta_{co}}) \in SE(3)$. Similarly, $g_{wc} = (p_{wc}, e^{\hat{\xi}\theta_{wc}})$ and $g_{wo} = (p_{wo}, e^{\hat{\xi}\theta_{wo}})$ denote rigid body motions from the world frame Σ_w to the camera

frame Σ_c and from the world frame Σ_w to the object frame Σ_o, respectively.

Position-based visual feedback control needs, in general, to derive the relative rigid body motion from image data. The relative rigid body motion from Σ_c to Σ_o can be led by using the composition rule for rigid body transformations [12] as follows:

$$g_{co} = g_{wc}^{-1} g_{wo}. \qquad (1)$$

The relative rigid body motion involves the velocity of each rigid body. To this aid, let us consider the velocity of a rigid body. We define the body velocity of the camera relative to the world frame Σ_w as $V_{wc}^b = [v_{wc}^T \; \omega_{wc}^T]^T$, where v_{wc} and ω_{wc} represent the velocity of the origin and the angular velocity from Σ_w to Σ_c, respectively [12].

Differentiating Eq. (1) with respect to time, the body velocity of the relative rigid body motion g_{co} can be written as follows (See [11]):

$$V_{co}^b = -\mathrm{Ad}_{(g_{co}^{-1})} V_{wc}^b + V_{wo}^b, \qquad (2)$$

where V_{wo}^b is the body velocity of the target object relative to Σ_w.

B. Image Features of Pinhole Camera Model

In this visual feedback system, we use the pinhole camera model with a perspective projection. Here, we consider $m(\geq 4)$ feature points on the rigid target object in this paper.

Let λ be a focal length, $p_{oi} \in \mathcal{R}^3$ and $p_{ci} \in \mathcal{R}^3$ be the position vectors of the target object's i-th feature point relative to Σ_o and Σ_c, respectively. We assume that multiple point features on a known object p_{oi} are given. The perspective projection of the i-th feature point onto the image plane gives us the image plane coordinate $f_i := [f_{xi} \; f_{yi}]^T \in \mathcal{R}^2$ as

$$f_i = \frac{\lambda}{z_{ci}} \begin{bmatrix} x_{ci} \\ y_{ci} \end{bmatrix}, \qquad (3)$$

where $p_{ci} = [x_{ci} \; y_{ci} \; z_{ci}]^T$. It is straightforward to extend this model to m image points by simply stacking the vectors of the image plane coordinate, i.e., $f(g_{co}) := [f_1^T \; \cdots \; f_m^T]^T \in \mathcal{R}^{2m}$. Hereafter, f_{ab} means $f(g_{ab})$ for simplicity.

C. Estimation Error System and Visual Motion Observer

In this subsection, we consider a nonlinear observer in order to estimate the relative rigid body motion g_{co} from the image feature f_{co}. Firstly, using Eq. (2), we choose estimates $\bar{g}_{co}$ and $\bar{V}_{co}^b$ of the relative rigid body motion and velocity, respectively as

$$\bar{V}_{co}^b = -\mathrm{Ad}_{(\bar{g}_{co}^{-1})} V_{wc}^b + u_e. \qquad (4)$$

The new input u_e is to be determined in order to drive the estimated values $\bar{g}_{co}$ and $\bar{V}_{co}^b$ to their actual values.

In order to establish the estimation error system, we define the estimation error between the estimated value $\bar{g}_{co}$ and the actual relative rigid body motion g_{co} as

$$g_{ee} = \bar{g}_{co}^{-1} g_{co}. \qquad (5)$$

We next define the error vector of the rotation matrix $e^{\hat{\xi}\theta_{ab}}$ as $e_R(e^{\hat{\xi}\theta_{ab}}) := \mathrm{sk}(e^{\hat{\xi}\theta_{ab}})^\vee$ where $\mathrm{sk}(e^{\hat{\xi}\theta_{ab}})$ denotes $\frac{1}{2}(e^{\hat{\xi}\theta_{ab}} - e^{-\hat{\xi}\theta_{ab}})$. Using this notation, the vector of the estimation error is given by $e_e := [p_{ee}^T \; e_R^T(e^{\hat{\xi}\theta_{ee}})]^T$.

Suppose the attitude estimation error θ_{ee} is small enough that we can let $e^{\hat{\xi}\theta_{ee}} \simeq I + \mathrm{sk}(e^{\hat{\xi}\theta_{ee}})$. Therefore, using a first-order Taylor expansion approximation, the estimation error vector e_e can be obtained from the image feature f_{co} and the estimated value of the relative rigid body motion $\bar{g}_{co}$ as follows:

$$e_e = J_e^\dagger(\bar{g}_{co})(f_{co} - \bar{f}_{co}), \qquad (6)$$

where $\bar{f}_{co}$ is an estimated value of the image feature and $J_e(\bar{g}_{co})$ is an image Jacobian-like matrix [11]. In the same way as Eq. (2), the estimation error system can be represented by

$$V_{ee}^b = -\mathrm{Ad}_{(g_{ee}^{-1})} u_e + V_{wo}^b. \qquad (7)$$

This estimation error system is passive from the input u_e to the output $-e_e$. Based on the passivity property, we consider the stabilizing control law as follows:

$$u_e = -K_e(-e_e), \quad K_e > 0. \qquad (8)$$

By the proposed visual motion observer constructed by Eqs. (4) and (8), the unmeasurable motion g_{co} will be exploited as the part of control law.

III. VISUAL MOTION OBSERVER-BASED SIMPLE POSE CONTROL

Although the time-varying desired motion is needed to the path planner, the desired motion in our previous works [10], [11] is assumed to be constant. Thus, we have to reconstruct the visual motion error system in order to handle the time-varying desired motion.

A. Pose Control Error System

Let us consider the pose control error system in order to achieve the control objective. First, we define the pose control error as follows:

$$g_{ec} = g_{cd}^{-1} g_{co}, \qquad (9)$$

which represents the error between the relative rigid body motion g_{co} and the reference one g_{cd}. It should be remarked that g_{co} can be calculated by using the estimated relative rigid body motion $\bar{g}_{co}$ and the estimation error vector $e_e = [p_{ee}^T \; e_R^T(e^{\hat{\xi}\theta_{ee}})]$ equivalently as follows:

$$g_{co} = \bar{g}_{co} g_{ee} \qquad (10)$$

$$\xi\theta_{ee} = \frac{\sin^{-1}\|e_R(e^{\hat{\xi}\theta_{ee}})\|}{\|e_R(e^{\hat{\xi}\theta_{ee}})\|} e_R(e^{\hat{\xi}\theta_{ee}}), \qquad (11)$$

although g_{co} cannot be measured directly [10]. Using the notation $e_R(e^{\hat{\xi}\theta})$, the vector of the pose control error is defined as $e_c := [p_{ec}^T \; e_R^T(e^{\hat{\xi}\theta_{ec}})]^T$.

Differentiating Eq. (9) with respect to time, the pose control error system can be represented as

$$V_{ec}^b = -\mathrm{Ad}_{(g_{ec}^{-1})}\Big(\mathrm{Ad}_{(g_{cd}^{-1})} V_{wc}^b + V_{cd}^b\Big) + V_{wo}^b, \quad (12)$$

where V_{cd}^b is the body velocity of the reference of the relative rigid body motion g_{cd}.

B. Visual Motion Error System and Stabilizing Control Law

Combining the estimation error system (7) and the pose control one (12), we construct the visual motion error system as follows:

$$\begin{bmatrix} V_{ec}^b \\ V_{ee}^b \end{bmatrix} = \begin{bmatrix} -\mathrm{Ad}_{(g_{ec}^{-1})} & 0 \\ 0 & -\mathrm{Ad}_{(g_{ee}^{-1})} \end{bmatrix} u + \begin{bmatrix} I \\ I \end{bmatrix} V_{wo}^b, (13)$$

where $u := [u_c^T \; u_e^T]^T$ and $u_c := \mathrm{Ad}_{(g_{cd}^{-1})} V_{wc}^b + V_{cd}^b$. Let us define the error vector of the visual motion error system as $x := [e_c^T \; e_e^T]^T$.

The passivity between the input u and the output $-x$ of the visual motion error system (13) is derived by using the following energy function

$$V(x) = \frac{1}{2}\|p_{ec}\|^2 + \phi(e^{\hat{\xi}\theta_{ec}}) + \frac{1}{2}\|p_{ee}\|^2 + \phi(e^{\hat{\xi}\theta_{ee}}),(14)$$

where $\phi(e^{\hat{\xi}\theta}) := \frac{1}{2}\text{tr}(I - e^{\hat{\xi}\theta})$ is the error function of the rotation matrix. Here, we consider the following control input

$$u = -K(-x)\nu, \quad K > 0. \quad (15)$$

By differentiating $V(x)$ along the trajectory of the system and using the control input u, the next equation is obtained if $V_{wo}^b = 0$ is satisfied.

$$\dot{V} = u^T(-x) = -x^T Kx. \quad (16)$$

Therefore, if $w = 0$, the equilibrium point $x = 0$ for the closed-loop system (13) and (15) is asymptotic stable, i.e., u is a stabilizing control law (15) for the system.

However, the stabilizing control law (15) is not based on optimization, the desired control performance cannot be guaranteed explicitly. In the next section, a stabilizing receding horizon control based on optimal control theory is proposed.

IV. VISUAL MOTION OBSERVER-BASED STABILIZING RECEDING HORIZON CONTROL

The objective of this section is to propose visual feedback control based on optimal control theory. A camera can provide more information than the current derivation from a nominal position at the sample instant. This property can be exploited to predict the target's future position and improve the control performance. In this section, we propose a stabilizing receding horizon control based on optimization.

A. Control Lyapunov Function

In this section, the finite horizon optimal control problem (FHOCP) for the visual motion error system (13) is considered. The FHOCP for the system (13) at time t consists of the minimization with respect to the input $u(\tau, x(\tau)), \tau \in [t, t+T]$, of the following cost function

$$J(x_0, u, T) = \int_t^{t+T} l(x(\tau), u(\tau))d\tau + F(x(t+T)) \quad (17)$$

$$l(x(t), u(t)) = E_{qc}(g_{ec}(t)) + E_{qe}(g_{ee}(t)) + u^T(t)R(t)u(t) \quad (18)$$

$$F(x) = \rho V(x), \quad q_{pi}(t) \geq 0, \quad q_{Ri}(t) \geq 0, \quad \rho > 0, \quad (19)$$

where $R(t)$ is a positive diagonal matrix, and $E_{qi}(g_{ei}(t)) := q_{pi}(t)\|p_{ei}(t)\|^2 + q_{Ri}(t)\phi(e^{\hat{\xi}\theta_{ei}(t)})$ $(i \in c, e)$, with the state $x(t) = x_0$. The speciality of the cost function (17)–(19) is that the terminal cost is derived from the energy function of the visual motion error system. Furthermore, the rotation error related part of the stage cost is derived from the error function $\phi(e^{\hat{\xi}\theta_{ab}})$ instead of the commonly used quadratic form $\|e_R(e^{\hat{\xi}\theta_{ab}})\|^2$. For a given initial condition x_0, we denote this solution of the FHOCP as $u^*(\tau, x(\tau)), \tau \in [t, t+T]$. In receding horizon control, at each sampling time δ, the resulting feedback control at state x_0 is obtained by solving the FHOCP and setting

$$u^{RH} := u^*(\delta, x_0). \quad (20)$$

A control Lyapunov function closely related to stability is defined as follows:

Definition 1 ([7]): A control Lyapunov function $S(x)$ is given by

$$\inf_u \left[\dot{S}(x) + l(x, u) \right] \leq 0, \quad (21)$$

where $l(x, u)$ is a positive definite function.

The following lemma concerning the control Lyapunov function is important to prove a stabilizing receding horizon control.

Lemma 1: Suppose that $V_{wo}^b = 0$, $\|\theta_{ec}\| \leq \frac{\pi}{2}$, $\|\theta_{ee}\| \leq \frac{\pi}{2}$ and the design parameter ρ satisfies

$$\rho^2 I \geq 4QR, \quad (22)$$

where $Q := \text{diag}\{q_{pc}I_3, q_{Rc}I_3, q_{pe}I_3, q_{Re}I_3\}$. Then, the energy function $\rho V(x)$ of the visual motion error system (13) can be regarded as a control Lyapunov function.

Proof: Using Eq. (16), which is the time derivative of V along the trajectory of the system (13), the positive definite function $l(x(t), u(t))$ (18) and the stabilizing control law u^k (15) with $K = \frac{\rho}{2}R^{-1}$ for the system, Eq. (21) can be transformed into

$$\inf_u [\dot{S}(x) + l(x, u)]$$
$$= \inf_u \left[\rho\dot{V} + E_{qc}(g_{ec}) + E_{qe}(g_{ee}) + u^T Ru \right]$$
$$= \inf_u \left[\left(u - \frac{\rho}{2}R^{-1}x\right)^T R \left(u - \frac{\rho}{2}R^{-1}x\right) - \frac{\rho^2}{4}x^T R^{-1}x \right.$$
$$\left. + E_{qc}(g_{ec}) + E_{qe}(g_{ee}) \right]$$
$$= -\frac{\rho^2}{4}x^T R^{-1}x + q_{pc}\|p_{ec}\|^2 + q_{Rc}\phi(e^{\hat{\xi}\theta_{ec}})$$
$$+ q_{pe}\|p_{ee}\|^2 + q_{Re}\phi(e^{\hat{\xi}\theta_{ee}})$$
$$\leq -\frac{\rho^2}{4}x^T R^{-1}x + q_{pc}\|p_{ec}\|^2 + q_{Rc}\|e_R(e^{\hat{\xi}\theta_{ec}})\|^2$$
$$+ q_{pe}\|p_{ee}\|^2 + q_{Re}\|e_R(e^{\hat{\xi}\theta_{ee}})\|^2$$
$$= -x^T \left(\frac{\rho^2}{4}R^{-1} - Q \right) x, \quad (23)$$

where we have used the fact that $\phi(e^{\hat{\xi}\theta_{ab}}) \leq \|e_R^T(e^{\hat{\xi}\theta_{ab}})\|$ for all $\|\theta_{ab}\| \leq \frac{\pi}{2}$. Therefore, the condition $\inf_u[\dot{S}(x) + l(x, u)] \leq 0$ will be satisfied, if the assumption $\rho^2 I \geq 4QR$. ∎

Lemma 1 shows the energy function $\rho V(x)$ of the visual motion error system (13) can be regarded as a control Lyapunov function in the case of $\rho^2 I \geq 4QR$.

B. Visual Motion Stabilizing Receding Horizon Control

Suppose that the terminal cost is the control Lyapunov function $\rho V(x)$, the following theorem concerning the stability of the receding horizon control holds.

Theorem 1: Consider the cost function (17)–(19) for the visual motion error system (13). Suppose that $V_{wo}^b = 0$, $\|\theta_{ec}\| \leq \frac{\pi}{2}$, $\|\theta_{ee}\| \leq \frac{\pi}{2}$, and $\rho^2 I \geq 4QR$, then the receding horizon control for the visual motion error system is asymptotically stabilizing.

Proof: Our goal is to prove that $J(x^*(t), u^{RH}, T)$, which is the cost-to-go applying the receding optimal control u^{RH}, will qualify as a Lyapunov function for the closed loop system. Construct the following suboptimal control strategy for the time interval $[t + \delta, t + T + \delta]$

$$\tilde{u} = \begin{cases} u^*(\tau) & \tau \in [t+\delta, t+T] \\ u^k(\tau) = \frac{\rho}{2}R^{-1}x & \tau \in [t+T, t+T+\delta] \end{cases} \quad (24)$$

where u^k is the stabilizing control law (15) with $K = \frac{\rho}{2}R^{-1}$ for the visual motion error system. The associated cost is

$$J(x^*(t+\delta), \tilde{u}, T)$$
$$= J(x(t), u^*, T) + \rho[V(x(t+T+\delta)) - V(x^*(t+T))]$$
$$- \int_t^{t+\delta} l(x^*(\tau), u^*)d\tau + \int_{t+T}^{t+T+\delta} l(x^*(\tau+T), u^k)d\tau, \quad (25)$$

where x^* is the optimal state trajectory. This cost, which is an upper bound for $J(x^*(t+\delta), u^*, T)$, satisfies

$$J(x^*(t+\delta), u^*, T) - J(x^*(t), u^*, T)$$
$$\leq \rho[V(x(t+T+\delta)) - V(x^*(t+T))]$$
$$- \int_t^{t+\delta} l(x^*(\tau), u^*)d\tau + \int_{t+T}^{t+T+\delta} l(x^*(\tau+T), u^k)d\tau. \quad (26)$$
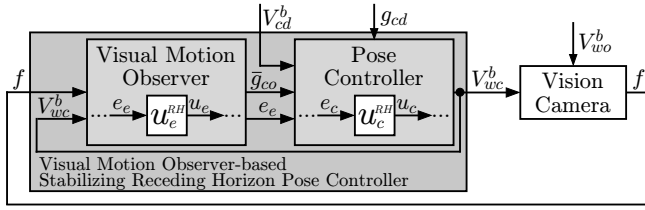
Fig. 2. Block diagram of visual motion stabilizing receding horizon control.

Using the positive definite function $l(x(t), u(t))$ (18) and the stabilizing control law u^k (15) for the system, and dividing both sides by δ and taking the limit as $\delta \to 0$, Eq. (26) can be transformed into

$$
\begin{aligned}
\lim_{\delta \to 0} & \frac{J(x^*(t+\delta), u^*, T) - J(x^*(t), u^*, T)}{\delta} \\
&\leq -\frac{\rho^2}{4} x^{*T}(t+T) R^{-1} x^*(t+T) + E_{qc}(g_{ec}^*(t+T)) \\
&\quad + E_{qe}(g_{ee}^*(t+T)) - x^{*T}(t) Q x^*(t) - u^{*T} R u^* \\
&\leq -x^{*T}(t+T) \left(\frac{\rho^2}{4} R^{-1} - Q \right) x^*(t+T) \\
&\quad - x^{*T}(t) Q x^*(t) - u^{*T} R u^*.
\end{aligned}
\tag{27}
$$

Considering that the control input during first δ is $u^{RH} = u^*$, by the assumption $\rho^2 I \geq 4QR$, the derivative of $J(x^*(t), u^{RH}, T)$ is negative definite. Therefore, we have shown that $J(x^*(t), u^{RH}, T)$ qualifies as a Lyapunov function and asymptotic stability is guaranteed. ∎

Theorem 1 guarantees the stability of the receding horizon control using the control Lyapunov function for the 3D visual motion error system (13) which is a highly nonlinear and relatively fast system. The block diagram of the visual motion stabilizing receding horizon control is shown in Fig. 2. Since the stabilizing receding horizon control design is based on optimal control theory, the control performance should be improved compared to the passivity-based simple pose control u^k (15), under the condition of adequate gain assignment in the cost function. It should be noted that the error function $\phi(e^{\hat{\xi}\theta_{ab}})$ of the rotation matrix can be directly used in the stage cost (18).

Remark 1: One of the contributions in this paper is that the proposed control law can be applied to the time-varying desired relative rigid body motion $g_{cd}(t)$, similar to in the case of the constant one.

V. IMAGE SPACE NAVIGATION FUNCTION-BASED PATH PLANNING

In [4], the inherent problem of the position-based visual feedback control by using only the error defined on the Cartesian space, is that the target object cannot always remain in the camera field of view during the servoing. Because the proposed stabilizing receding horizon control in the previous section is the position-based method, it may leave the camera field of view. In this section, a path planner to be appropriate for the visual motion error system is designed through an image space navigation function to guarantee to keep all features into the camera field of view. The control objective in this paper is stated as follows:

Control Objective: The vision camera follows the target object, i.e., the relative rigid body motion $g_{co}(t)$ is coincided with the time-varying desired one $g_{cd}(t)$, which is generated to keep all features into the camera field of view and converges the final desired one g_{cd_f}.

From the proposed stabilizing receding horizon control law for the visual motion error system, the input to vision camera is designed as follows:

$$
V_{wc}^b = \text{Ad}_{(g_{cd})} \left(u_c^{RH} - V_{cd}^b \right),
\tag{28}
$$

where $u^{RH} = [(u_c^{RH})^T \ (u_e^{RH})^T]^T$. Hence, the vision camera input is only needed the body velocity V_{cd}^b of the reference of the relative rigid body motion g_{cd}[1].

Here, we introduce the navigation function-based method as a technique for constructing artificial potential fields in order to design V_{cd}^b which can achieve the control objective. Firstly, we define the desired image feature vector and the final one as $f_{cd} := f(g_{cd})$ and $f_{cd_f} := f(g_{cd_f})$, respectively. The navigation functions used in this paper are defined as follows:

Definition 2 ([6],[13]): Let D be a space where all feature points of the target remain visible, and let f_{cd_f} be in the interior of D. A map $\varphi : D \to [0, 1]$ is a navigation function if it is
1) smooth on D (at least a $C^{(2)}$ function);
2) a unique minimum exists at f_{cd_f};
3) admissible on D, i.e., uniformly maximal on the boundary of D;
4) a Morse function.

A. Path Planning of Desired Body Velocity

To develop the desired body velocity V_{cd}^b, we derive a relationship between f_{cd} defined on the image space and V_{cd}^b defined on the Cartesian space. Differentiating Eq. (3), we have the following relation between the desired feature point p_{cd_i} and the body velocity V_{cd}^b:

$$
\dot{p}_{cd_i} = e^{\hat{\xi}\theta_{cd}} \begin{bmatrix} I & -\hat{p}_{o_i} \end{bmatrix} V_{cd}^b.
\tag{29}
$$

Moreover, the relation between the desired image feature f_{cd_i} and the desired feature point p_{cd_i} can be expressed as

$$
\dot{f}_{cd_i} = \begin{bmatrix} \frac{\lambda}{z_{cdi}} & 0 & -\frac{\lambda x_{cdi}}{z_{cdi}^2} \\ 0 & \frac{\lambda}{z_{cdi}} & -\frac{\lambda y_{cdi}}{z_{cdi}^2} \end{bmatrix} \dot{p}_{cd_i}.
\tag{30}
$$

Hence, the desired image feature vector and the desired body velocity can be related as

$$
\dot{f}_{cd} = J_L(g_{cd}) V_{cd}^b,
\tag{31}
$$

where $J_L(g_{cd}) : SE(3) \to \mathcal{R}^{2m \times 6}$ is defined as

$$
J_L(g_{cd}) := \begin{bmatrix} J_{L1}^T(g_{cd}) & J_{L2}^T(g_{cd}) & \cdots & J_{Lm}^T(g_{cd}) \end{bmatrix}^T
\tag{32}
$$

$$
J_{Li}(g_{cd}) := \begin{bmatrix} \frac{\lambda}{z_{cdi}} & 0 & -\frac{\lambda x_{cdi}}{z_{cdi}^2} \\ 0 & \frac{\lambda}{z_{cdi}} & -\frac{\lambda y_{cdi}}{z_{cdi}^2} \end{bmatrix} e^{\hat{\xi}\theta_{cd}} \begin{bmatrix} I & -\hat{p}_{oi} \end{bmatrix},
$$
$$
(i = 1, \cdots, m).
\tag{33}
$$

Inspired by Eq. (31) and the definition of the navigation function, the desired body velocity V_{cd}^b is designed as follows:

$$
V_{cd}^b = -k_{cd} J_L^\dagger(g_{cd}) \nabla \varphi,
\tag{34}
$$

where $\nabla \varphi(f_{cd}) := \left(\frac{\partial \varphi(f_{cd})}{\partial f_{cd}} \right)^T$ denotes the gradient vector of $\varphi(f_{cd})$ and $k_{cd} \in \mathcal{R}$ is the positive gain. The design of the image navigation function $\varphi(f_{cd})$ is considered in the next subsection. Substituting (34) into (31), the velocity of the desired image feature vector yields

$$
\dot{f}_{cd} = -k_{cd} J_L(g_{cd}) J_L^\dagger(g_{cd}) \nabla \varphi.
\tag{35}
$$

Here, it is assumed that $\nabla \varphi(f_{cd}) \notin NS(J_L^T(f_{cd}))$ where $NS(\cdot)$ denotes the null space operator, similar to [6]. Since f_{cd} is chosen a priori via the off-line path planning routine in (35), this assumption can be satisfied.

---

[1]The relative rigid body motion g_{cd} can be obtained solving $\dot{g}_{cd} = g_{cd} V_{cd}^b$.

B. Image Space Navigation Function

In this subsection, we develop the image space navigation function $\varphi(f_{cd})$ [5], [6]. Here, the image space navigation function is designed that all image features keep into visible set.

Firstly, we define two auxiliary functions $\eta(f_{cd}) : \mathcal{R}^{2m} \to [-1, 1]^{2m}$ and $s(\eta) : [-1, 1]^{2m} \to \mathcal{R}^{2m}$ as follows:

$$\eta(f_{cd}) = \mathrm{diag} \left\{ \frac{2}{f_{x_M} - f_{x_m}}, \frac{2}{f_{y_M} - f_{y_m}}, \cdots \frac{2}{f_{y_M} - f_{y_m}} \right\} f_{cd}$$
$$- \left[\frac{f_{x_M} + f_{x_m}}{f_{x_M} - f_{x_m}} \quad \frac{f_{y_M} + f_{y_m}}{f_{y_M} - f_{y_m}} \quad \cdots \quad \frac{f_{y_M} + f_{y_m}}{f_{y_M} - f_{y_m}} \right]^T \quad (36)$$

$$s(\eta) = \left[\frac{\eta_1 - \eta_{f1}}{(1 - \eta_1^{2\kappa})^{\frac{1}{2\kappa}}} \quad \cdots \quad \frac{\eta_{2m} - \eta_{f2m}}{(1 - \eta_{2m}^{2\kappa})^{\frac{1}{2\kappa}}} \right]^T, \quad (37)$$

where $\eta(f_{cd}) = [\eta_1(f_{cd}) \ \eta_2(f_{cd}) \ \cdots \ \eta_{2m}(f_{cd}) \ ]^T$ and $\kappa > 0 \in \mathcal{R}$ is an additional parameter to change the potential field. $\eta(f_{cd_f}) = [\eta_{f1}(f_{cd}) \ \eta_{f2}(f_{cd}) \ \cdots \ \eta_{f2m}(f_{cd}) \ ]^T :$ $\mathcal{R}^{2m} \to [-1, 1]^{2m}$ is defined as same as (36). f_{x_M}, f_{x_m}, f_{y_M} and $f_{y_m} \in \mathcal{R}$ denote the maximum and minimum pixel values along the x- and y-axis, respectively. η and s are the functions in order to normalize the current pixel value for the maximum and minimum pixel values, and to define the error between the current image feature and the final one, respectively. Then, the model space navigation function $\tilde{\varphi}(\eta) \in \mathcal{R}^{2m} \to [0, 1]$ is defined as

$$\tilde{\varphi}(\eta) := \frac{\bar{\varphi}}{1 + \bar{\varphi}}. \quad (38)$$

Moreover, the objective function $\bar{\varphi}(\eta) \in \mathcal{R}^{2m} \to \mathcal{R}$ is defined as

$$\bar{\varphi}(\eta) := \frac{1}{2} s^T(\eta) K_s s(\eta), \quad (39)$$

where $K_s \in \mathcal{R}^{2m \times 2m}$ is a positive definite symmetric matrix.

The image space navigation function denoted by $\varphi(f_{cd}) \in D \to \mathcal{R}$, can be developed as follows:

$$\varphi(f_{cd}) := \tilde{\varphi} \circ \bar{\varphi} \circ s \circ \eta(f_{cd}), \quad (40)$$

where $\circ$ denotes the composition operator. The gradient vector $\nabla \varphi(f_{cd})$ can be represented as

$$\nabla \varphi(f_{cd}) := \left(\frac{\partial \varphi}{\partial f_{cd}} \right)^T$$
$$= \frac{s^T K_s}{(1 + \bar{\varphi})^2} \times \mathrm{diag} \left\{ \frac{1 - \eta_1^{2\kappa-1} \eta_{f1}}{(1 - \eta_1^{2\kappa})^{\frac{2\kappa+1}{2\kappa}}}, \quad \cdots \quad \frac{1 - \eta_{2m}^{2\kappa-1} \eta_{f2m}}{(1 - \eta_{2m}^{2\kappa})^{\frac{2\kappa+1}{2\kappa}}} \right\}$$
$$\times \mathrm{diag} \left\{ \frac{2}{f_{x_M} - f_{x_m}}, \frac{2}{f_{y_M} - f_{y_m}}, \cdots, \frac{2}{f_{y_M} - f_{y_m}} \right\}. \quad (41)$$

It should be noted that $f_{cd} \to f_{cd_f}$ from (36)–(41) when $\nabla \varphi(f_{cd}) \to 0$.

C. Convergence Analysis of Path Planner

Suppose that $\nabla \varphi(f_{cd})$ is not a member of the null space $J_L^T(f_{cd})$, the following theorem concerning the convergence of the path planner holds.

Theorem 2: Suppose that $\nabla \varphi(f_{cd}) \notin NS(J_L^T(f_{cd}))$ and the initial desired image feature vector $f_{cd}(0)$ satisfies $f_{cd}(0) \in D$. Then, the desired image feature vector (35) ensures that $f_{cd}(t) \in D$ and has the asymptotically stable equilibrium point f_{cd_f}.

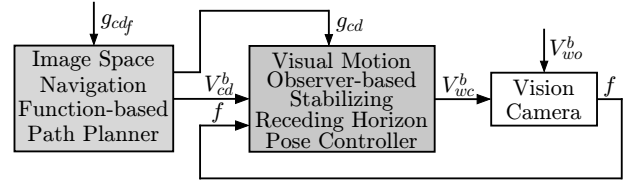*Proof:* Consider the following positive definite function:

Fig. 3. Block diagram of visual motion stabilizing receding horizon control with image space navigation function-based path planner.

$$V_n(f_{cd}(t)) = \varphi(f_{cd}(t)). \quad (42)$$

Evaluating the time derivative of $V_n(f_{cd})$ along the trajectories of Eq. (35) gives us

$$\dot{V}_n(f_{cd}(t)) = (\nabla \varphi)^T \dot{f}_{cd}$$
$$= -k_{cd} (\nabla \varphi)^T J_L(g_{cd}) J_L^\dagger(g_{cd}) \nabla \varphi$$
$$= -k_{cd} (J_L^T \nabla \varphi)^T (J_L^T J_L)^{-1} J_L^T \nabla \varphi$$
$$\leq -\underline{k} \| J_L^T \nabla \varphi \|^2, \quad (43)$$

where we use the property $\underline{k} \| a \|^2 \leq k_{cd} a^T (J_L^T J_L)^{-1} a$, $\forall a \in \mathcal{R}^6$ and $\underline{k}$ denotes a positive constant. It is clear from Eq. (43) that $V_n(f_{cd})$ is a non-increasing function in the sense that

$$V_n(f_{cd}(t)) \leq V_n(f_{cd}(0)). \quad (44)$$

From Eqs. (42) and (44), the condition $f_{cd}(t) \in D$, $\forall t > 0$ is satisfied for any initial condition $f_{cd}(0) \in D$. By following LaSall's Theorem [14], it can be proved that the only invariant set that satisfies $\| J_L^T(f_{cd}) \nabla \varphi(f_{cd}) \| = 0$ is the origin. Considering the assumption $\nabla \varphi(f_{cd}) \notin NS(J_L^T(f_{cd}))$, we have shown that $\| \nabla \varphi(f_{cd}) \| = 0$. Therefore, it can be concluded that $f_{cd} \to f_{cd_f}$ from Sec V-B. ∎

Theorem 2 guarantees the convergence of the time-varying desired image feature vector $f_{cd}(t)$ to the final one f_{cd_f}. The path planner can be designed to keep all features into the camera field of view based on the image space navigation function. The block diagram of the visual motion stabilizing receding horizon control with the image space navigation function-based path planner is shown in Fig. 3.

Although position-based control can allow feature points to leave the field of view, the principle advantage of it is that it is possible to describe tasks in terms Cartesian pose as is common in many applications, e.g., robotics [1], and that it does not need a desired image a priori. Thus, the proposed method which is connected the position-based receding horizon control and the image-based path planner allows us to extend technological application area. The main contribution of this paper is to show that the path planner which always remains in the camera field of view during the servoing is designed for the position-based visual feedback receding horizon control based on optimal control theory.

Remark 2: It is also interesting to note that the Jacobian $J_L(\cdot)$ between the image feature vector and the body velocity is exactly the same form as the Jacobian $J_e(\cdot)$ for the estimation error which is derived using a first Taylor expansion approximation.

Remark 3: Our previous work has proposed the stabilizing receding horizon control for visual feedback systems with the manipulator dynamics [10]. In a similar way, our proposed approach can be applied to robot systems which have to be controlled with a small sampling period.
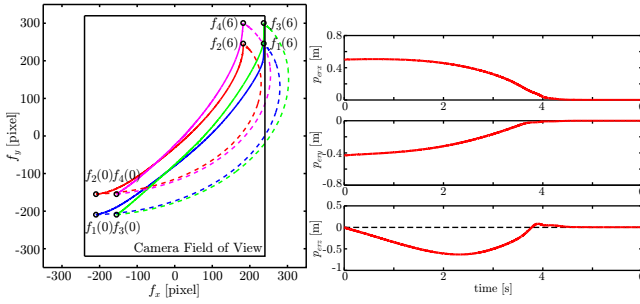
Fig. 4. Trajectory of image feature points f_{co}: Solid; with proposed method: Dashed; with previous one.

Fig. 5. Pose control translational error p_{er}.

VI. SIMULATION RESULTS

In this section, we present simulation results for the visual feedback control with the path planner via the image space navigation function, compared with the simple constant desired motion proposed in [10]. The control objective is that the vision camera tracks the static target object to keep all target feature points (four points) inside the camera field of view. In other words, it is bring the actual relative rigid body motion $g_{co}(t)$ to a given reference one g_{cd_f} using a time-varying reference one $g_{cd}(t)$, and it can be achieved to make both the estimation and the pose control errors zero.

The simulation is carried out with the initial condition $p_{co} = [0.2 \ 0.2 \ -1.35]^T$ m, $\xi\theta_{co} = [0 \ 0 \ 0]^T$ rad. The final desired relative rigid body motion is $p_{cd_f} = [-0.23 \ -0.3 \ -1.35]^T$ m, $\xi\theta_{cd_f} = [0 \ 0 \ \pi/2]^T$ rad. This condition means that the vision camera moves from end to end of the field of view diagonally with optical axis rotation. To solve the real time optimization problem, the software C/GMRES [15] is utilized. The control input with the receding horizon control is updated every 2 ms. It must be calculated by the receding horizon controller within that period. The horizon was selected as $T = 0.02$ s.

The simulation results are presented in Figs. 4 and 5. Fig. 4 shows the trajectory of image feature points f_{co}. In Fig. 4, the solid lines denote the trajectory applying the proposed stabilizing receding horizon control with the path planner, and the dashed lines denote those for the simple constant desired value, respectively. $f_{co}(0) := [f_1(0) \ f_2(0) \ f_3(0) \ f_4(0)]$ and $f_{co}(6) := [f_1(6) \ f_2(6) \ f_3(6) \ f_4(6)]$ shows the values of the image feature vector in the case of the initial condition and those of in the case of $t = 6$ s, respectively. The control method have to be designed that the feature points do not get out of the camera field of view which is denoted as the rectangle in Fig. 4. From Fig. 4, it is concluded that the proposed method can make the vision camera keep all feature points in the field of view. Although the convergence to the desired values is also achieved in the case of the previous method [10] in the simulation, it corresponds to fail in the actual experiment as the vision camera miss the target object.

Fig. 5 shows the actual translational control error p_{er}, which is the position error vector between the current relative rigid body motion $g_{co}(t)$ and the final desired one g_{cd_f}, instead of the time-varying desired one $g_{cd}(t)$. It should be noted that the position error with z-axis increases, while the

ones with x-axis and y-axis are monotonically decreasing. This means that the vision camera moves away once in order to keep the target object. This validates one of the expected advantages of the stabilizing receding horizon control with the path planner for the visual feedback system.

VII. CONCLUSIONS

This paper proposes a stabilizing receding horizon control via an image space navigation function for a 3-D eye-in-hand visual feedback system, which are highly nonlinear and relatively fast system. The main contribution of this paper is to show that the path planner which always remains in the camera field of view during the servoing is designed for the position-based visual feedback receding horizon control based on optimal control theory. Especially, our proposed method does not need a desired image a priori. Simulation results are presented to verify the control performance with visibility maintenance of the proposed control scheme and the previous one [10].

REFERENCES

[1] F. Chaumette and S. A. Hutchinson, "Visual Servoing and Visual Tracking," In:B. Siciliano and O. Khatib (Eds), *Springer Handbook of Robotics*, Springer–Verlag, pp. 563–583, 2008.

[2] N. R. Gans and S. A. Hutchinson, "Stable Visual Servoing through Hybrid Switched-System Control," *IEEE Trans. on Robotics*, Vol. 23, No. 3, pp. 530–540, 2007.

[3] V. Lippiello, B. Siciliano and L. Villani, "Position-based Visual Servoing in Industrial Multirobot Cells using a Hybrid Camera Configuration," *IEEE Trans. on Robotics*, Vol. 23, No. 1, pp. 73–86, 2007.

[4] F. Chaumette, "Potential Problems of Stability and Convergence in Image-based and Position-based Visual Servoing," D. J. Kriegman, G. D. Hager and A. S. Morse (Eds.), *The Confluence of Vision and Control, Lecture Notes in Control and Information Sciences 237*, Springer–Verlag, pp. 66–78, 1998.

[5] N. J. Cowan, J. D. Weingarten and D. E. Koditschek, "Visual Servoing via Navigation Functions," *IEEE Trans. Robotics and Automation*, Vol. 18, No. 4, pp. 521–533, 2002.

[6] J. Chen, D. M. Dawson, W. E. Dixon and V. K. Chitrakaran, "Navigation Function-based Visual Servo Control," *Automatica*, Vol. 43, No. 7, pp. 1165–1177, 2007.

[7] D. Q. Mayne, J. B. Rawlings, C. V. Rao and P. O. M. Scokaert, "Constrained Model Predictive Control: Stability and Optimality," *Automatica*, Vol. 36, No. 6, pp. 789–814, 2000.

[8] M. Sauvée, P. Poignet, E. Dombre and E. Courtial, "Image based Visual Servoing through Nonlinear Model Predictive Control," *Proc. 45th IEEE Conference on Decision and Control*, pp. 1776–1781, 2006.

[9] G. Allibert, E. Courtial and Y. Touré, "Visual Predictive Control for Manipulators with Catadioptric Camera," *Proc. 2008 IEEE International Conference on Robotics and Automation*, pp. 510–515, 2008.

[10] T. Murao, H. Kawai and M. Fujita "Predictive Visual Feedback Control with Eye-in/to-Hand Configuration via Stabilizing Receding Horizon Approach," *Proc. of the 17th IFAC World Congress on Automatic Control*, pp. 5341–5346, 2008.

[11] M. Fujita, H. Kawai and M. W. Spong, "Passivity-based Dynamic Visual Feedback Control for Three Dimensional Target Tracking: Stability and L_2-gain Performance Analysis," *IEEE Trans. on Control Systems Technology*, Vol. 15, No. 1, pp. 40–52, 2007.

[12] R. Murray, Z. Li and S. S. Sastry, *A Mathematical Introduction to Robotic Manipulation*, CRC Press, 1994.

[13] E. Rimon and D. E. Koditschek, "Exact Robot Navigation using Artificial Potential Functions," *IEEE Trans. Robotics and Automation*, Vol. 8, No. 5, pp. 501–518, 1992.

[14] H. K. Khalil, *Nonlinear Systems* (3rd ed.), Prentice Hall, 2002.

[15] T. Ohtsuka, "A Continuation/GMRES Method for Fast Computation of Nonlinear Receding Horizon Control," *Automatica*, Vol. 40, No. 4, pp. 563–574, 2004.